

Enhanced detection of unknown defect patterns on wafer bin maps based on an open-set recognition approach

Jin-Su Shin ^{a,b}, Min-Joo Kim ^{a,b}, Beom-Seok Kim ^c, Dong-Hee Lee ^{c,*,1}

^a Department of Semiconductor and Display Engineering, Sungkyunkwan University, 2066, Seobu-ro, Suwon-si, Gyeonggi-do 16419, Republic of Korea

^b Memory Division, Samsung Electronics Co., Ltd., 1-1 Samsungjeonja-ro, Hwaseong-si, Gyeonggi-do 18448, Republic of Korea

^c Department of Industrial Engineering, Sungkyunkwan University, 2066, Seobu-ro, Suwon-si, Gyeonggi-do 16419, Republic of Korea



ARTICLE INFO

Keywords:

Wafer-bin map classification
Real field data
Unknown defect patterns
One-class SVM
Open-set recognition

ABSTRACT

It is crucial to detect and classify defect patterns on wafers in semiconductor-manufacturing processes for wafer-quality management and prompt analysis of defect causes. In recent years, continuous technological innovation and advancements in semiconductor-industry processes have led to an increase in unknown defect patterns, which must be detected and classified. However, detection of unknown defect patterns is difficult due to complex reasons, such as training on non-existent defect classes, closed datasets owing to industrial security, and labeling large volumes of manufacturing data. Owing to these challenges, methods for detecting unknown defect patterns in an actual semiconductor-manufacturing environment primarily rely on qualitative indicators, such as intuition and experience of engineers. To overcome these problems, this study proposes a methodology based on open-set recognition to accurately detect unknown defect patterns. This methodology begins with two preprocessing steps: constrained mean filtering (C-mean filtering); and Radon transform to diminish noise and efficiently extract features from wafer-bin maps. This study then develops an entropy-estimation one-class support vector machine (EEOC-SVM), which accounts for the uncertainty in the one-class SVM classification results. EEOC-SVM computes entropy-uncertainty scores based on the distance between decision boundaries and samples and then reclassifies uncertain samples using a weighted sum of uncertainties for each class. This method can effectively detect unknown defect patterns. The proposed method achieves a detection performance of over 98 % for various defect classes based on experiments conducted with new defect patterns occurring in actual semiconductor-manufacturing environments. These results confirm that the proposed method is an effective tool for detecting and addressing unknown defect patterns.

1. Introduction

The semiconductor-manufacturing industry is the cornerstone of modern technology. A variety of processes are used to imprint numerous elements onto a single chip to manufacture integrated circuits capable of processing and storing complex functions. In this process, wafer bin maps (WBM), which visualize the results of electrical die tests, are widely used for analyzing and measuring wafer defects (Kyeong and Kim, 2018). Defect patterns detected in the WBM contain information for analyzing various causes of wafer defects, such as process failures, production-equipment abnormalities, and design flaws. Therefore, accurate classification and analysis of the defect patterns in the WBM can play a crucial role in identifying the specific processes or machines that

cause defects.

Recent trends in semiconductor research have aimed to enhance chip processing power and functionality by integrating an increasing number of devices into a single chip. Consequently, with the introduction of the latest process technologies and a variety of new equipment, semiconductor manufacturing processes have become more refined and advanced, and unknown defect patterns that differ from traditional defect types are constantly emerging. However, identification of emerging defect patterns and labeling of data still rely heavily on qualitative metrics, such as engineer intuition and judgment (C. Y. Hsu et al., 2020). If engineers fail to identify defects based on intuition and experience, the risk of reliability and quality issues in semiconductor production increase significantly, which has a considerable impact on

* Corresponding author.

E-mail address: dhee@skku.edu (D.-H. Lee).

¹ ORCID: 0000-0001-8549-8992

wafer-manufacturing costs (J. Zhu et al., 2022). Therefore, the accurate classification of unknown WBM defect patterns is critical (F.-L. Chen and Liu, 2000; S. C. Hsu and Chien, 2007).

It is significantly difficult for newly discovered unknown defect patterns to predict their shape or timing in advance. Moreover, research on the detection of unknown defect patterns in the WBM is compounded by closed datasets owing to industrial security, high costs and time required to label vast amounts of manufacturing data, and the difficulty in acquiring unknown defect data. Consequently, traditional classification algorithms or classifiers that consider only the known defect patterns included in the training data have limitations in detecting these unknown defect patterns (T. Kim and Behdinan, 2023). Despite this background, most WBM defect-analysis studies primarily focus on the classification accuracy and speed of known defect types and fail to provide solutions for detecting unknown defect patterns (Cha and Jeong, 2022; Chen et al., 2022; E. S. Kim et al., 2021; M. Kim et al., 2023; Nag et al., 2022; Nakazawa and Kulkarni, 2018; Shinde et al., 2022; Xu et al., 2022; N. Yu et al., 2019). Recent studies introduce models to improve the detection performance of mixed defects based on known defect patterns (Hou et al., 2024; Zhang et al., 2024), or propose augmentation methods utilizing vision transformer models, a cutting-edge deep learning model, to address the problem of imbalance between known defect classes (Fan and Chiu, 2024). However, research on detecting unknown defect patterns in WBM is relatively scarce. Some studies highlighted the potential occurrence of unknown defect patterns in the WBM and their associated risks, underscoring the importance of research in this area. However, these studies only offer limited solutions for detecting unknown defect patterns, such as presuming a certain shape of potentially unknown defect-pattern classes (Lee and Kim, 2020), setting a classifier's threshold to reject samples with high uncertainty (M. B. Alawieh, 2020), or training on both out-of-distribution (OOD) and in-distribution (IND) defects present in the training data to detect a limited number of OOD defects (Y. Kim, 2020). This implies that a comprehensive solution capable of effectively detecting entirely new types of defects without any prior information on unknown defect patterns has not yet been presented.

Therefore, this study aims to accurately detect unknown defect patterns using an open-set recognition (OSR) methodology based on an entropy-estimation one-class support vector machine (EEOC-SVM) to overcome the limitations of existing research. This methodology effectively removes noise from WBM without compromising the key defect areas by incorporating preprocessing steps such as constrained mean filtering (C-mean filtering) and Radon transform, and efficiently extracts the core features of WBM defects. Additionally, by utilizing the radial basis function (RBF) kernel embedding of an OC-SVM trained only on known defect patterns, previously undefined defect patterns can be successfully detected. Additionally, in order to minimize errors arising from binary classification based on the learned boundary of the OC-SVM, the distance between the sample and boundary was calculated to estimate the probability of each sample belonging to each region, and the entropy was calculated. Adjustment of the classification results to maximize the weighted sum of uncertainties for highly uncertain samples enables the successful detection of previously undefined defect patterns while also enabling more accurate discrimination of samples prone to misclassification.

This remainder of this paper is structured as follows. In Section 2, we review recent trends in assumed unknown defect patterns in WBM classification research and various feature-extraction methods. In Section 3, we explain the EEOC-SVM-based OSR methodology. In Section 4, we introduce the WM-811K dataset used in the study and verify the effectiveness of the methodology through experimental results and analysis using the WM-811K data. Section 5 demonstrates the practical applicability of the proposed method by using real industrial data containing unknown defect patterns. Finally, Section 6 concludes the paper and briefly outlines future research directions. The experimental results show that the proposed methodology effectively detects previously

undefined defect patterns with high accuracy compared with existing classification techniques. In particular, the EEOC-SVM has shown significant performance, even in environments where multiple unknown defect patterns occur simultaneously and has been proven to be effective in classifying various types of defects. This implies that the EEOC-SVM may be a useful tool for detecting unpredictable defect types in semiconductor-manufacturing processes.

2. Related works

2.1. Open-set recognition

OSR aims to identify or reject unknown classes based on existing classes. To achieve this, OSR utilizes various methods of dimensionality reduction and embedding of the original data to analyze the differences from known classes. This enables the effective rejection or identification of unknown classes.

Early work on OSR involved thresholding the post-SoftMax output of a deep-learning model to classify samples below a certain probability as unknown classes (Nguyen et al., 2015). However, this approach is limited because the threshold may not be appropriately applied. Therefore, the pre-SoftMax technique, which uses an adjustable threshold for the logit value before the SoftMax layer, and Open-Max (Bendale and Boult, 2016) method, which utilizes extreme probability values of samples based on the Weibull distribution of each class, have been proposed.

These approaches can be effectively applied to analyze the various defect patterns that may arise with the advancement of semiconductor processes (Júnior et al., 2016; Mahdavi and Carvalho, 2021). However, in wafer-defect analysis studies, the lack of diverse defect data owing to security reasons and the difficulty in distinguishing between defect patterns pose challenges. Despite the importance of exploring unknown defect patterns, successful application of OSR in this field has been limited, with only a few studies partially applying OSR techniques.

For example, (M. B. Alawieh, 2020) attempted to maintain the performance of classifiers by adding a rejection option for samples with low confidence. However, their focus was on predefined defect patterns, leading to decreased recall performance and issues with rejecting samples from known defect pattern classes. (Frittoli et al., 2022) proposed a method using a wafer defect map (WDM) with a VGG-based submanifold sparse convolutional network (SSCN) for dimensionality reduction, followed by the use of a pretrained Gaussian mixture model (GMM) to determine unknown classes based on density-based likelihood scores. However, this approach has limitations, such as lengthy weight-learning processes, significant impact of threshold settings, increased cost for effective VGG training-data augmentation, and restricted performance-evaluation metrics for defect recall.

Therefore, our study aims to present a methodology for defect detection in WBM using OSR techniques, focusing on effectively detecting previously unseen defect patterns by leveraging only known defect classes and patterns in limited scenarios.

2.2. Unknown defect patterns on wafer bin maps

Most research on detecting and classifying defects in WBMs focuses on using pre-prepared training data and labels for supervised learning (Cha and Jeong, 2022; Chen et al., 2022; E. S. Kim et al., 2021; M. Kim et al., 2023; Nag et al., 2022; Nakazawa and Kulkarni, 2018; Shinde et al., 2022; Xu et al., 2022; N. Yu et al., 2019), unsupervised learning that does not require labels for all training data (Wu et al., 2015; Lee et al., 2021), and semi-supervised learning that optimizes the efficiency and cost of labeling the training data (Lee and Kim, 2020; Shim et al., 2020; Yu and Liu, 2021). These approaches concentrate primarily on building classifiers based on previously acquired training data to detect known defect patterns. Given the increasing importance of detecting unknown defect patterns in WBM analysis due to the miniaturization of

semiconductor manufacturing processes, several studies have acknowledged the challenge of identifying new types of defects that are not predefined in traditional supervised-learning models (Batoool et al., 2021). This lack of research can lead to difficulties in responding when unknown defect patterns emerge. Therefore, this section aims to understand the necessity of this study by identifying the research mentioned in WBM studies on the detection issues of unknown defect patterns, their solutions, and the limitations of these studies.

The studies that mentioned problems with unknown defect patterns are summarized in Table 1. For example, (Y. Kim, 2020) highlighted that the classifiers used in previous supervised research could not detect unknown defect types, leading to misclassification and performance degradation. To address this, a method was proposed to differentiate between OOD and IND defects by dividing the entire training dataset and training different losses for each dataset. However, this approach requires predefined OOD and IND defect patterns, which necessitates data collection and training. Furthermore, (H. Lee and Kim, 2020) proposed a multi-label classification solution based on 16 complex defect patterns assumed from four single defect types ('Circle', 'Scratch', 'Partial Ring', 'Local Zone'), aiming to classify unlearned complex defect types. However, this method has limitations in detecting new single-defect patterns or unlabeled defect types. (M. B. Alawieh, 2020) introduced a selective-learning technique to prevent the performance degradation of supervised learning-based convolutional neural network (CNN) classifiers owing to the emergence of unknown defect patterns, where the classifier does not judge samples that do not meet the decision threshold. However, this approach relies on a user-defined hyperparameter for the threshold, which significantly reduces the recall performance of the classifier for known defect patterns. Finally, (Nakazawa and Kulkarni, 2019) suggested a rule-based feature-extraction method to isolate areas of interest in WBM defect regions and eliminate noise, and they proposed that they could extract the core patterns of unlearned defect patterns. However, this research, which used a rule-based methodology, is limited in its application to 'random' defect patterns and requires further classification and validation after simple feature extraction.

Consequently, although some studies have proposed solutions for the problem of unknown defect patterns in WBMs, a truly effective method for detecting new types of defects without any prior information about these unknown defect patterns has not yet been introduced. Therefore, in this study, we propose a methodology that introduces an OSR solution for effectively detecting unknown defect patterns in WBMs.

Table 1
Studies with assumptions about unknown defect patterns in WBMs.

Reference	Objective	Algorithm	Model
(Y. Kim, 2020)	OOD detection	OOD detection (Supervised learning)	CNN
(H. Lee and Kim, 2020)	Classification of mixed patterns	Multi-label classification (Supervised learning)	Semi-supervised convolutional deep generative model with multiple discriminative networks
(M. B. Alawieh, 2020)	Prevent misclassification of unknown defect pattern	Deep selective learning (Supervised learning)	CNN & Auto encoder
(Nakazawa and Kulkarni, 2019)	Feature extraction of defect patterns	Feature extraction (Segmentation)	Seg-net & U-net & Fully convolutional network
Proposed	Detecting and preventing misclassification of unknown defect patterns	OSR (Unsupervised learning)	EEOC-SVM

2.3. Feature-extraction method for wafer bin maps

In OSR methodologies, various discrimination strategies are primarily based to the distance between the input images. To successfully apply this approach, the input images must be appropriately mapped to a pre-trained latent space, enabling effective calculation of the distances between each image (Mahdavi and Carvalho, 2021). During this process, the choice of dimensionality-reduction technique is of utmost importance. Features with an excessively high dimension may experience reduced accuracy in distance-based classification and increased computational costs. Conversely, excessively reducing dimensionality can risk losing essential information from the original data. Therefore, features must be extracted with appropriate dimensions that preserve the critical characteristics of the original data while ensuring computational efficiency. Various dimensionality-reduction techniques used in WBM research have been investigated, ranging from rule-based manual feature-extraction methods to dimension-extraction methods using end-to-end structured CNNs.

Table 2 illustrates different feature-extraction techniques. These are broadly classified into two categories: manual feature-extraction methods and automated end-to-end feature-extraction approaches (Kang and Kang, 2021). Manual methods include geometric feature extraction, density-based feature extraction, and feature extraction using the Radon transform. Geometric feature (Wu et al., 2015) extraction utilizes parameters such as the long axis, short axis, area, curvature, and radius to analyze the shapes of defects. Density-based feature extraction (Saqlain et al., 2019) divides the wafer into multiple regions and transforms the defect count within each region into a histogram for model training. In addition, Radon transform-based feature extraction (Wu et al., 2015) is an important method that uses the sinogram obtained from the Radon transform of WBM images to identify the core areas of the WBM. Other studies have also analyzed the

Table 2
Feature-extraction techniques used in WBM research.

Reference	Feature Extract Method	Feature Size	Classifier	Algorithm
(Wu et al., 2015)	Geometry, Radon, 18 Transform	116 (40 Geometry) $\times 2$ (Median Filter)	SVM	Classification (Supervised Learning)
(J. Yu and Lu, 2016)	Geometry, Radon Transform, Gray, Texture	53 (24 Radon, 18 Geometry, 6 Gray, 5 Texture)	Joint local and nonlocal linear discriminant analysis-based Fisher discriminant	SVM
(J. Zhu et al., 2022)	Geometry, Density	17 (13 Density, 4 Geometry)	SVM	
(Piao et al., 2018)	Radon Transform	30 (30 Radon)	Ensemble (4 Decision tree Models)	
(Saqlain et al., 2019)	Geometry, Density, Radon Transform	66 (40 Radon, 20 Density, 6 Geometry)	Ensemble (Linear regression, Random forest, Gradient boosting machine, Feedforward neural network)	
(Kang and Kang, 2021)	Geometry, Density, Radon Transform & CNN	59 (40 Radon, 13 Density, 6 Geometry) & (64,64)	Ensemble (Feedforward neural networks, CNN)	
Proposed	Radon Transform	20 (20 Radon)	EEOC-SVM	OSR (Unsupervised)

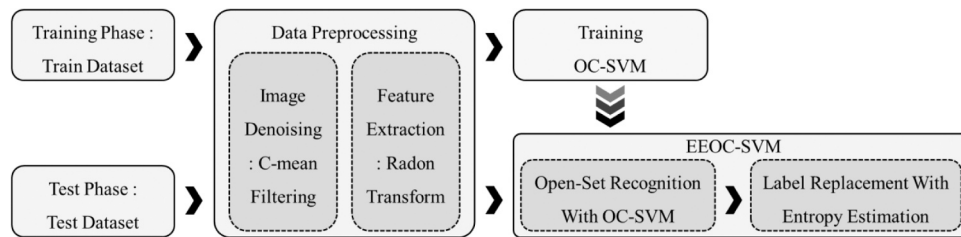


Fig. 1. Overall framework of the proposed method.

grayscale values or texture characteristics of images (J. Yu and Lu, 2016).

Automated end-to-end feature-extraction methods that utilize weight values from deep-learning models, such as CNNs and auto-encoders, have also been widely used (Kang and Kang, 2021). These feature-extraction methods primarily aim to efficiently use known patterns for accurate classification and are generally focused on supervised-learning research. However, the effectiveness of these feature-extraction methods has not been fully verified in studies aimed at detecting unknown patterns. Therefore, this study aims to train the proposed EEOC-SVM classifier using features obtained through the Radon transform, while also evaluating the performance of various feature-extraction methods used in WBM research.

3. Proposed method

Fig. 1 illustrates the comprehensive framework of the methodology proposed in this study. The training dataset consists of samples with known defect patterns, whereas the test dataset is assumed to include both potentially unknown and known types of defect patterns. The objective of this study is to accurately classify whether the samples in the test dataset are known defective patterns or not. During the learning and testing phases, each dataset underwent common preprocessing. The preprocessed training dataset was used to train the OC-SVM, and this trained OC-SVM is then applied to perform OSR on the preprocessed test dataset. Subsequently, the predicted sample-classification labels were re-assigned through an entropy-estimation process using the EEOC-SVM module, leading to the derivation of the final classification results of the samples.

Proposed Method Overview

The training phase of the methodology proposed in this study is as follows:

- (1) **Data Preprocessing:** First, all samples in the training data were subjected to noise reduction using a C-mean filter. Subsequently, important features are extracted through the Radon transform. This preprocessing stage helps extract meaningful information from the data and reduce unnecessary variability.
- (2) **Training OC-SVM:** The OC-SVM was trained using only known types of defect-pattern data. The OC-SVM employs a RBF kernel to map the data into a higher-dimensional space and form a boundary that distinguishes data belonging to the normal category from anomalies based on the distribution of the data.

The testing stage of the methodology proposed in this study is conducted through data preprocessing (1) and EEOC-SVM (2)–(3). The specific procedures are as follows:

- (1) **Data Preprocessing:** The samples in the test dataset underwent the same preprocessing steps as those in the training phase.
- (2) **OSR with OC-SVM:** The decision boundary of the OC-SVM trained from the training data was used as a reference to perform binary classification on each sample of the test data. The distances between each sample and the decision boundary were then calculated. This distance information is used to quantify the uncertainty in the classification results for each sample using information entropy.
- (3) **Label Replacement:** The quantified classification-uncertainty score for each sample is used to calculate a weighted sum by class, which is then used to determine the final classification label for the sample. This process allows for a more accurate detection of known and unknown defect-pattern samples.

Fig. 2 shows the classification flow of test data after assuming the 'Scratch' defect pattern in the WM-811K data set as an unknown defect pattern.

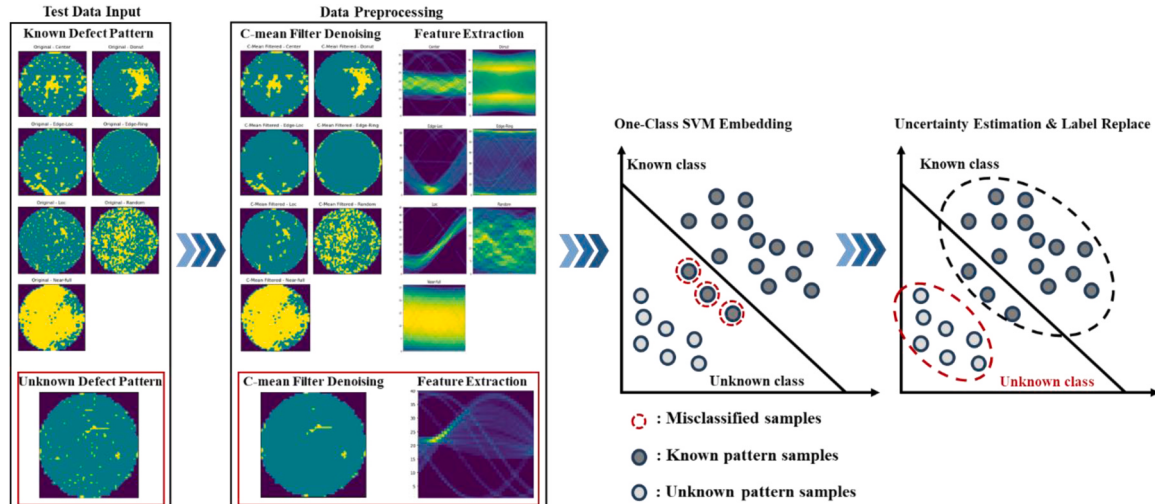


Fig. 2. Flow diagram of the proposed method in the test phase.

3.1. Data preprocessing: C-mean Filtering

In this study, a C-mean filter was utilized to filter out noise in the WBM images. Noise filtering is commonly employed in image-classification research to eliminate unnecessary regions and focus on essential core patterns, thereby significantly reducing the computational complexity (Hyun and Kim, 2020). In the WBM analysis, some chips with defects may influence the extraction of defective pattern characteristics; hence, such chips are considered noise and are removed before

$$Bin(P_i) = \begin{cases} 2 & \text{if } \frac{1}{|n_i|} \sum_{j \in n_i} Bin(P_j) \geq t_c \\ 1 & \text{Otherwise} \end{cases} \quad \text{for } i \in P_{def} \quad (1)$$

ALGORITHM 1. : C-Mean Filter for Defect Pattern Detection

```

# Inputs:
#   - Image: Input image of wafer map (defect: 2, normal: 1)
#   - Neighborhood Size: Size of the neighborhood for pixel analysis ( $N_{size} = 3$ )
#   - Edge Threshold: Threshold value for detecting edges ( $\mathcal{E} = 1.25$ )

# Initialize:
#   -  $\delta$  : Half of the  $N_{size}$ 
#   -  $Img_{filtered}$  : Defect patterns removed from the original image
#   -  $N_{valid}$  : Indicates the number of valid neighboring pixels
#   -  $N$  : Each k-neighbor pixel within the neighborhood

1. for each pixel (i, j) in the image do
2.   If pixel value  $Img[i, j] == 2$  then
3.      $N_{valid} = [] \leftarrow$  Reset valid neighbor pixels
4.     for each  $N \leq N_{size}$  do
5.        $N_{valid} \leftarrow$  add( $Img[i + \delta_i, j + \delta_j]$ )
6.     End for
7.   If  $N_{valid} \neq 0$  then:
8.      $N_{Mean} \leftarrow \frac{N_{valid}}{N_{size}}$ 
9.     If  $N_{Mean} \leq \mathcal{E}$  then
10.       $Img_{filtered} \leftarrow 1$ 
11. End for
12. Output:  $Img_{filtered}$ 

```

extracting the features of defective patterns. While the Median filter technique, the most common and straightforward method, has been predominantly used in most WBM studies (S. Chen et al., 2022; Liao et al., 2014; Piao et al., 2018; Wu et al., 2015; J. Yu and Lu, 2016), it has the drawback of removing chips that form defect patterns, such as Edge-Ring and Scratch, owing to excessive noise removal. This is shown in Fig. 3(b).

In contrast, the C-mean filter used in this study targets only the surrounding areas of each defect pattern to identify edges and remove noise, effectively preserving linear patterns. This can be observed in Fig. 3(c). The working principle of the C-mean filter is presented in Algorithm 1. If the threshold of the condition is not met, the bin data of the chip change the pixel value to 1 ('None' pattern), considering it as noise, as shown in Eq. (1). This approach contributes to the efficient removal of unnecessary information from the WBM image analysis and more accurately extracts the characteristics of essential defect patterns.

3.2. Data preprocessing: radon transform

The Radon transform is a useful tool for analyzing and understanding complex 2D data. It has been widely used in WBM research to handle 2D images, particularly as a method for feature extraction, considering the characteristics of the original images (Table 2). The Radon transform effectively represents the characteristics of defect patterns by utilizing the distance from the origin and angle information with respect to the x-axis on the wafer map, making it suitable for extracting and learning defects. In this study, the feature-extraction method using the Radon transform is as follows. First, the equation of a line with an angle θ from the x-axis and a distance ρ from the origin can be expressed as Eq. (2)

$$x \cos \theta + y \sin \theta = \rho \# \quad (2)$$

For a specific (ρ, θ) , if we denote the result after applying the Radon transform as $g(\rho, \theta)$, and the element in the x-th row and y-th column of the WBM as $M(x, y)$, then $g(\rho, \theta)$ can be expressed as Eq. (3)

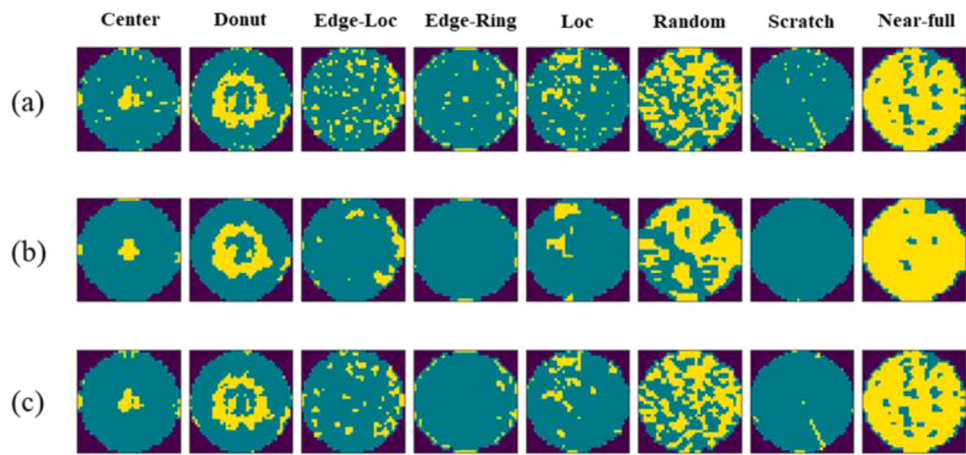


Fig. 3. WM-811K defect pattern images: (a) original images (b) median-filtering applied (c) c-mean filtering applied.

$$g(\rho, \theta) = \sum_{x=1}^m \sum_{y=1}^n \mathbf{M}(x, y) \delta(x \cos \theta + y \sin \theta - \rho) \# \quad (3)$$

In formula (4) $\delta(k)$ is an impulse function that has a value of 1 only when $(k=0)$. In the WBM analysis, it plays an important role in selecting the data points of each defective die that correspond to a straight line at a certain angle. Utilizing this function, the location and distribution of defective dies can be accurately determined under certain conditions, which is useful for failure analysis and defect pattern recognition.

$$\delta(k) = \begin{cases} 1, \text{if } k = 0 \\ 0, \text{otherwise} \end{cases} \# \quad (4)$$

The values obtained by varying ρ, θ can be represented in matrix form \mathbf{G} , and the results of transforming WBM into ρ, θ axes are shown in Fig. 4(a). Fig. 4(b) shows the result after the Radon transformation of the WBM following C-mean filtering, where the characteristics of each defect pattern are emphasized, and noise that may hinder learning is removed.

$$\mathbf{G} = \begin{pmatrix} g(1, 1) & g(1, 2) & \cdots & g(1, \theta_{180}) \\ g(2, 1) & g(2, 2) & \cdots & g(2, \theta_{180}) \\ \vdots & \vdots & \ddots & \vdots \\ g(\rho_{\max}, 1) & g(\rho_{\max}, 2) & \cdots & g(\rho_{\max}, \theta_{180}) \end{pmatrix}, \mathbf{G}_\mu = \begin{pmatrix} g_\mu(1) \\ g_\mu(2) \\ \vdots \\ g_\mu(\rho_{\max}) \end{pmatrix} \# \quad (5)$$

Finally, using formula (5), a new column vector \mathbf{G}_μ was obtained, consisting of the averages of each row of the matrix \mathbf{G} derived from the Radon transform. To extract the necessary features for training from the column vector \mathbf{G}_μ , 20 Radon-based features were extracted using cubic interpolation. The extracted 20-dimensional feature vector was then used to train the decision boundary of the OC-SVM and classify the samples.

3.3. Training OC-SVM

SVM, which is among the most popular methodologies in traditional machine-learning-based OSR approaches (Geng et al., 2021; Mahdavi

and Carvalho, 2021), was utilized to apply the OSR technique for detecting unknown defect patterns. In particular, the OC-SVM is an optimized model for binary classification based on whether the test data match a known defect pattern. OC-SVM utilizes kernel functions for mapping data to a higher-dimensional space and forms a decision boundary that encompasses as much normal data as possible while being as far away from the origin as possible. The formula of the objective function is shown in Eq. (6), and the variables used in the OC-SVM formula are listed in Table 3.

$$\min_{\mathbf{w}, \xi_i, \rho} \frac{1}{2} \|\mathbf{w}\|^2 + \frac{1}{\nu l} \sum_{i=1}^l \xi_i - \rho \# \quad (6)$$

subject to $(\mathbf{w} \bullet \Phi(\mathbf{x}_i)) \geq \rho - \xi_i, \quad \xi_i \geq 0 \text{ for all } i = 1, 2, \dots, l$

This process involves defining a Lagrangian function using the method of Lagrange multipliers (Eq. (7)) and applying the Karush–Kuhn–Tucker conditions by differentiating with respect to variables \mathbf{w}, ξ , and ρ (Eqs. (8)–(10)):

$$L_p = \frac{1}{2} \|\mathbf{w}\|^2 + \frac{1}{\nu l} \sum_{i=1}^l \xi_i - \rho - \sum_{i=1}^l \alpha_i (\mathbf{w} \bullet \Phi(\mathbf{x}_i) - \rho + \xi_i) - \sum_{i=1}^l \beta_i \xi_i \# \quad (7)$$

$$\frac{\partial L_p}{\partial \mathbf{w}} = \mathbf{w} - \sum_{i=1}^l \alpha_i \Phi(\mathbf{x}_i) = 0 \quad \therefore \mathbf{w} = \sum_{i=1}^l \alpha_i \Phi(\mathbf{x}_i) \# \quad (8)$$

$$\frac{\partial L_p}{\partial \xi_i} = \frac{1}{\nu l} - \alpha_i - \beta_i = 0 \quad \therefore \alpha_i = \frac{1}{\nu l} - \beta_i \# \quad (9)$$

$$\frac{\partial L_p}{\partial \rho} = -1 + \sum_{i=1}^l \alpha_i = 0 \quad \therefore \sum_{i=1}^l \alpha_i = 1 \# \quad (10)$$

Subsequently, the Lagrange multipliers are calculated and transformed into a dual problem, as shown in Eq. (11), from which the final objective function that forms the decision boundary of the OC-SVM is derived:

$$\min \frac{1}{2} \sum_{i=1}^l \sum_{j=1}^l \alpha_i \alpha_j \Phi(\mathbf{x}_i) \Phi(\mathbf{x}_j) \# \quad (11)$$

In this study, we only used data from known defect patterns in the

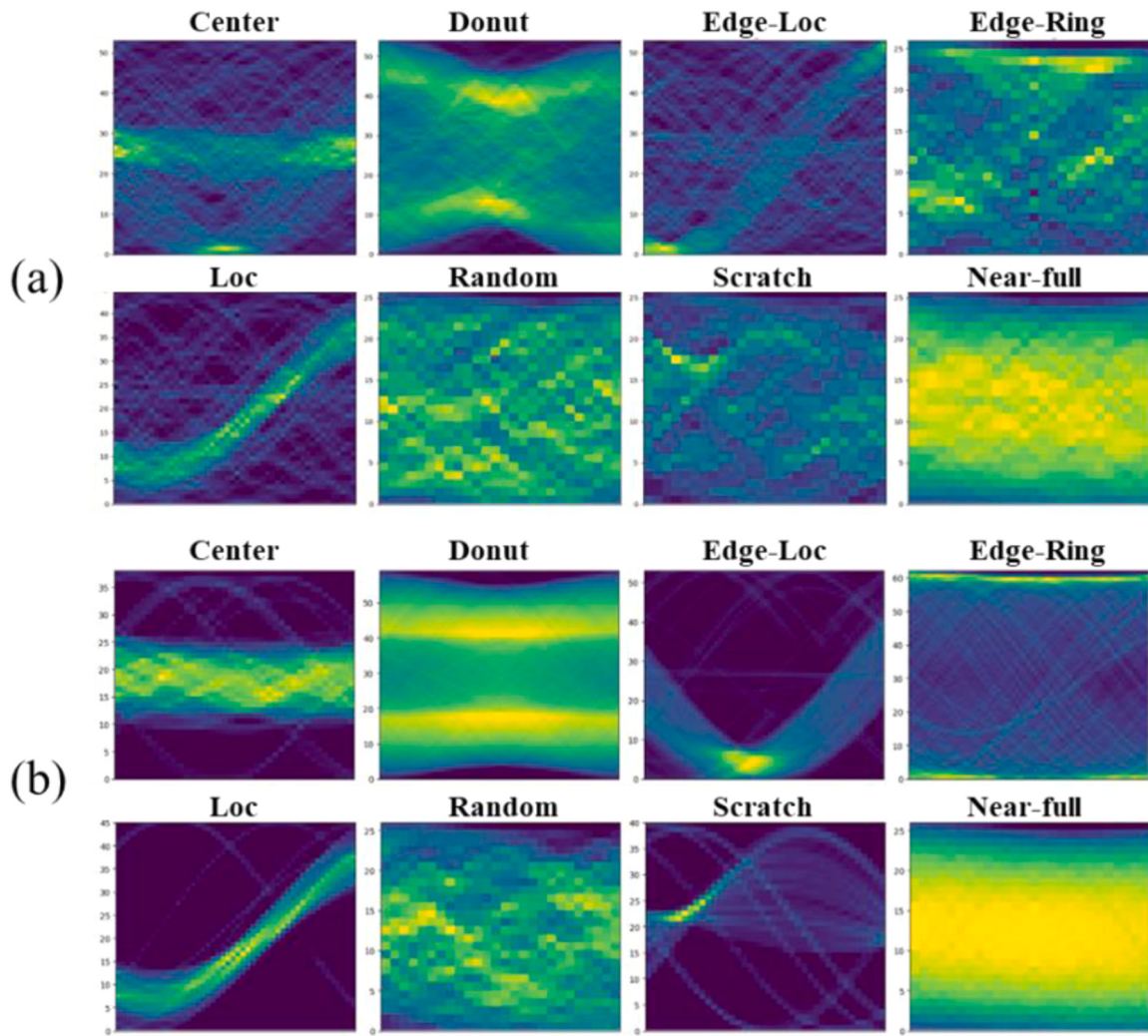


Fig. 4. Defect pattern-image sinogram (a) before filtering (b) after filtering.

Table 3
Variables used for formulating OC-SVM.

Symbol	Description	Value
x	Input data	$x \in \mathbb{R}^p$
w	Vector representing the direction of the hyperplane	$w \in \mathbb{R}^q$
ϕ	Mapping function (Data to feature space)	$\mathbb{R}^p \rightarrow \mathbb{R}^q$
l	Number of samples (Known defect patterns)	$l \in \{1, \dots, l\}$
ν	Ratio of support vectors used for model training (Hyperparameter)	$0 < \nu < 1$
ξ	Distance from hyperplane to outlier samples	$\xi \in \mathbb{R}$
ρ	Distance from origin to hyperplane	$\rho \in \mathbb{R}$
α_i	Lagrange multiplier for each samples point	$0 \leq \alpha_i \leq \frac{1}{\nu l}$
β_i	Kernel function parameters	$\beta_i > 0$

training phase to form a decision boundary using the RBF kernel to determine whether a sample belongs to an unknown or known class. In reality, known classes do not consist of a single class but of several predefined defect pattern classes. These known defect pattern classes were merged into a single dataset, which was subsequently used to train the model and generate a decision boundary through unsupervised learning, as shown in Fig. 5.

3.4. Label replacement with entropy estimation

The EEOC-SVM method proposed in this study represents a new

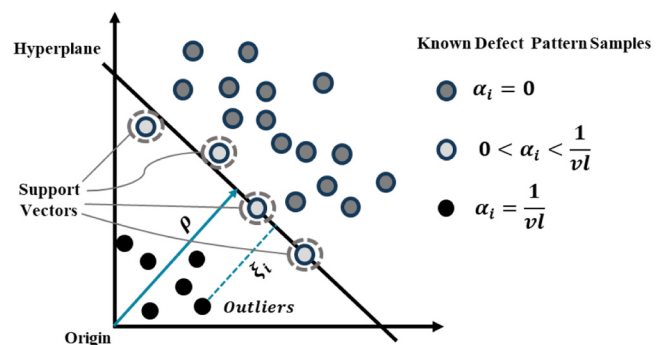


Fig. 5. Decision boundary of OC-SVM trained by known defect patterns.

attempt to enhance the performance of the traditional OC-SVM. Traditionally, the OC-SVM relies on a hyperplane derived from training data to determine whether new data belong to a specific class. However, this approach depends on the hyperplane and cannot solve the misclassification issue arising from the limitations of the training data (F. Zhu et al., 2016). To address this issue, we introduced an entropy-estimation method to quantify the uncertainty of each sample and conducted additional analyses on samples with high uncertainty.

The purpose of EEOC-SVM is to utilize the decision boundary of OC-SVM to estimate the uncertainty of the probability that each sample

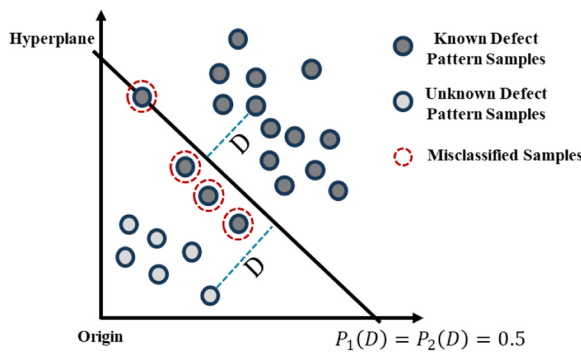


Fig. 6. Estimation of probability of sample using distance from trained decision boundary.

belongs to either a known class or an unknown class, and to appropriately replace the labels of samples with high classification uncertainty. In this study, we calculated the probability values to measure uncertainty using the distance D between data points and the decision boundary. The distance D between data points and the decision boundary was obtained using the decision function value of the OC-SVM. The decision function is calculated as shown in Eq. (12), where α_i are the learned Lagrange multipliers, K is the RBF kernel function representing the similarity between the training data point x_i and the test data point x . Finally, the model's bias ρ indicates the distance between the origin and the decision boundary. Therefore, as shown in Fig. 6, this method represents the distance (D) between each sample and the trained boundary of the OC-SVM. Consequently, test data points with high similarity to the training data, which belong to the known class, will have positive distance values, while test data points with low similarity will have negative distance values.

Eq. 13 shows the process of calculating the probability that a data point belongs to either a known or unknown class using the distance D between the decision boundary and the data point. By setting the probability of data points on the decision boundary to 0.5, Minmax scaling is applied such that positive distance values are scaled to probabilities between 0.5 and 1, and negative distance values are scaled to probabilities between 0 and 0.5. The resulting value can be interpreted as the probability that the data point belongs to the known class, defined as $P_1(D)$. Conversely, $1-P_1(D)$ is the probability that the data point belongs to the unknown class, defined as $P_2(D)$.

$$D = \sum_{i=1}^l \alpha_i K(x_i, x) - \rho \# \quad (12)$$

Table 4
Distribution of each defect pattern type in WM-811K.

Defect Pattern	Number of Samples
Center	4294
Donut	555
Edge-Loc	5189
Edge-Ring	9680
Loc	3593
Random	866
Scratch	1193
Near-full	149
None	145,861
Total	171,380

$$P_1(D) = \begin{cases} \text{MinMax}(0.5, 1) & (D > 0) \\ 0.5 & (D = 0) \\ \text{MinMax}(0, 0.5) & (D < 0) \end{cases} \# \quad (13)$$

$$P_1(D) = P(\text{Sample belonging to a known class})$$

$$P_2(D) = 1 - P_1(D) = P(\text{Sample belonging to an unknown class})$$

In Eq. (14), the entropy $H(D)$ measures the uncertainty of the classification result for each sample. The entropy $H(D)$ utilizes $P_1(D)$ and $P_2(D)$ as defined in Eq. (13). Consequently, the information entropy in Eq. (14) quantifies the uncertainty of the classification result by calculating the probability $P_1(D)$ of a sample belonging to the Known class and the probability $P_2(D)$ of belonging to the Unknown class, using the distance D from the decision boundary of the trained OC-SVM. In EEOC-SVM, uncertainty is calculated for all test data samples, and the top 5% of samples with the highest uncertainty are selected for further analysis.

$$H(D) = -\{P_1(D)\log_2 P_1(D) + P_2(D)\log_2 P_2(D)\} \# \quad (14)$$

For these selected samples, a k-nearest neighbor (KNN) algorithm based on cosine similarity is applied. Subsequently, the class weights of the nearest neighbors obtained as a result are aggregated, and the class with the greatest sum of weights is reassigned to the sample. In this process, to assign lower weights to samples with higher uncertainty, the entropy values are multiplied by -1 . Through this procedure, our study aims to enhance the performance of the OC-SVM, particularly by improving the classification accuracy of data with high uncertainty. Algorithm 2 describes the process of applying the KNN algorithm to data with high entropy values to aggregate the class weights of the nearest neighbors and reassign the labels of the data.

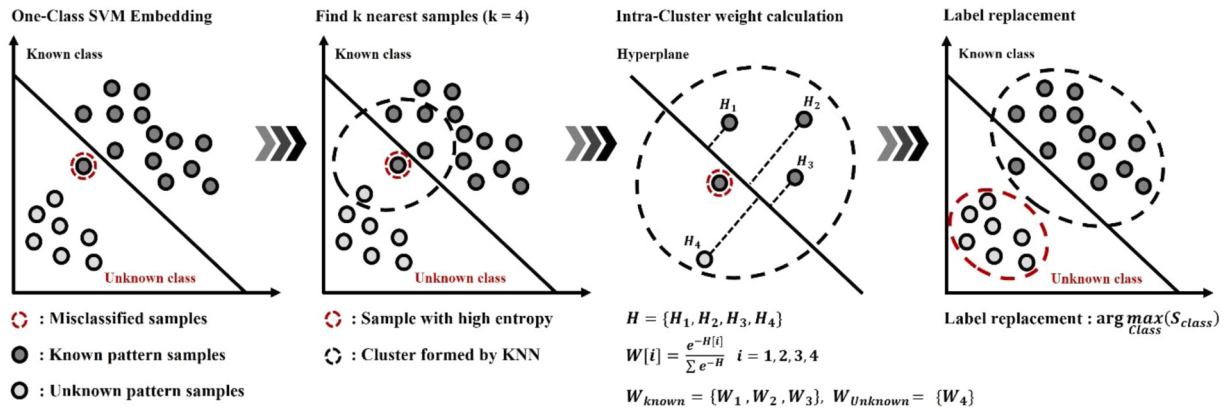


Fig. 7. Method for reassigning labels of misclassified samples in EEOC-SVM.

ALGORITHM 2. : EEOC-SVM Label Replacement with Weighted Sum of Information Entropy

3.5. Experimental design

The WM-811K dataset is extensively used in WBM defect analyses.

```

# Inputs:
# -  $\mathcal{X}_{test}$  Feature values of the data used to evaluate the model
# -  $\mathcal{Y}_{pred}$ : The classification prediction results of OC-SVM on the test dataset
# -  $\mathcal{E}$  : Information entropy value calculated based on each sample's distance from the boundary of the SVM
# -  $\mathcal{C}$ : Entropy percentile, samples with entropy above this value are considered high-entropy samples (95%)
# -  $\mathcal{N}_{test}$  : Total Number of  $\mathcal{X}_{test}$  samples
# -  $\mathcal{D}$  : Calculated distance of  $\mathcal{X}_{test}$  samples using cosine similarity

# Initialize:
# -  $\mathcal{N}_{size}$  : The number of nearest neighbours in  $\mathcal{X}_{test}$  with the highest cosine similarity
# -  $\mathcal{E}_H$ : Indices where  $\mathcal{E}$  values are greater than  $\mathcal{C}$ 
# -  $\mathcal{H}$  : Set of entropies of selected nearby samples
# -  $W[i]$  : Weight value of the i-th element in set  $\mathcal{H}$ 
# -  $S_{class}$ : Weighted sum value for each class

#High-entropy sample detection start code
1. for each  $Idx$  in  $\mathcal{N}_{test}$  do
2.   If  $\mathcal{E}[idx] \geq \mathcal{C}$  then
3.      $\mathcal{E}_H \leftarrow Add(Idx)$ 
4.      $\mathcal{H} \leftarrow Add(\mathcal{E}[idx])$ 

#Determine the new predicted value by applying the weighted sum of the entropy
5. for each  $Idx$  in  $\mathcal{E}_H$  do
6.    $\mathcal{N} \leftarrow$  A List of  $\mathcal{N}_{size}$  nearest neighbors with 'cosine similarity'
7.    $\mathcal{N}_{idx} \leftarrow$  Index list of  $\mathcal{N}$ 
8.    $W[i] \leftarrow \frac{e^{-H[\mathcal{N}_{idx}]}}{\sum_{idx} e^{-H[\mathcal{N}_{idx}]}}$  Calculate the weight value for each neighbor sample
9.    $S_{class} = \{ \}$ 
10.  for  $i$  in  $\mathcal{N}_{idx}$  do
11.    if  $\mathcal{Y}_{pred}[i]$  not in  $S_{class}$  then
12.       $S_{class}[\mathcal{Y}_{pred}[i]] \leftarrow 0$  Initialize the sum value for each class if not already present
13.       $S_{class}[\mathcal{Y}_{pred}[i]] \leftarrow S_{class}[\mathcal{Y}_{pred}[i]] + W[i]$  Update the weight sum of each class
14.    end for
# Select the class with the highest weighted sum value
15.     $\mathcal{Y}_{new}[Idx] \leftarrow \text{Arg max}_{class}(S_{class})$ 
16. end for

```

This method can improve the performance of the OC-SVM and enhance the classification accuracy for data with high uncertainty. Such an approach is especially meaningful for imbalanced datasets and contributes to reducing the performance degradation due to misclassification. Fig. 7 shows the process of replacing the classes of misclassified samples using the proposed EEOC-SVM, based on the decision boundary of OC-SVM.

Case Study 1: using WM-811K dataset

This dataset comprises eight defect patterns (Center, Donut, Edge-Loc, Edge-Ring, Loc, Random, Scratch, and Near-Full) and one normal pattern (None). The number of samples for each defect pattern and the images for each defect pattern are shown in Table 4 and Fig. 8, respectively. The primary aim of this study is to accurately identify unknown defect patterns in the test data that are not present in the training data. Therefore, to simulate the emergence of unknown defect patterns that are not included in the training data, we masked each of the eight defect patterns in the WM-811K dataset using a 'leave-one-out' approach, as shown in Fig. 8. We then divided the remaining defect patterns into training and test datasets. Finally, we added the previously

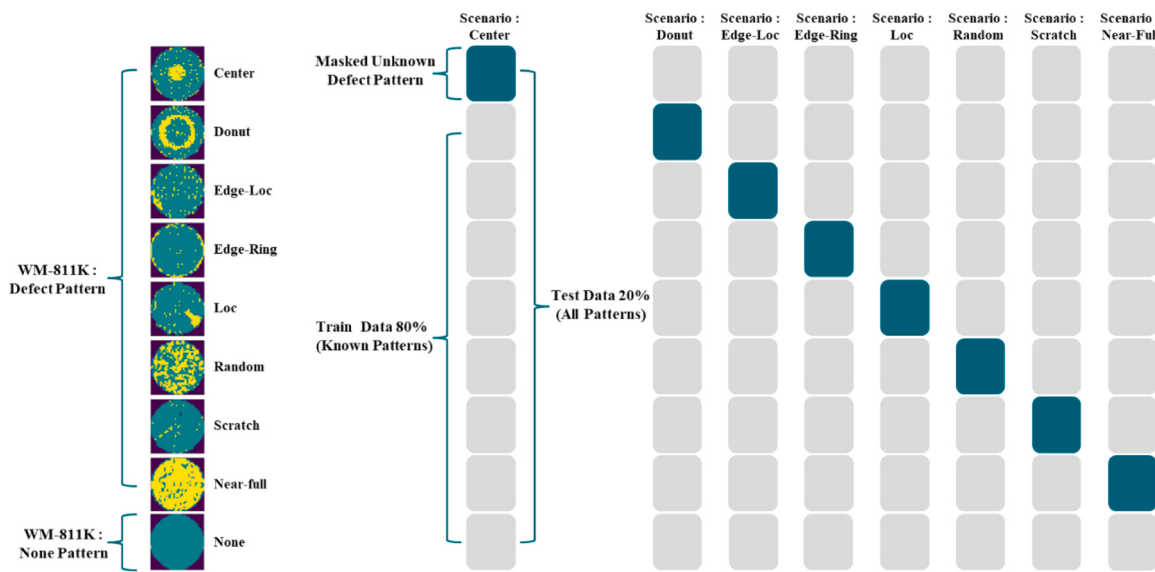


Fig. 8. Dataset-construction process used in the study.

Confusion Matrix		Model Predicted label	
		Negative (Known Pattern)	Positive (Unknown Pattern)
True Label	Negative (Known Pattern)	True Negative	False Positive
	Positive (Unknown Pattern)	False Negative	True Positive

Fig. 9. Confusion matrix of study.

Table 5
Performance of the proposed model: Accuracy & Recall.

Scenario Name	Accuracy	Recall
Center	0.94	0.90
Donut	0.94	1.00
Edge-Loc	0.88	0.48
Edge-Ring	0.94	0.95
Loc	0.90	0.54
Random	0.94	1.00
Scratch	0.91	0.21
Near-full	0.94	1.00
Average (Macro)	0.92	0.76

masked and excluded defect pattern data into the test dataset only. Using these data sets, we designed experiments to evaluate the performance of the proposed model to accurately distinguish between known and unknown defect patterns in test data.

3.6. Experimental results of proposed method

In this study, we propose a methodology and EEOC-SVM to accurately distinguish between known and unknown defect patterns. To validate the effectiveness of this research, as shown in Fig. 8, each defect pattern in the WM-811K dataset was assumed as an unknown pattern, and the classification performance of the evaluation dataset was measured using models trained on each scenario. The metrics used for performance evaluation were the overall data classification accuracy and the recall metric for unknown defect patterns (Eq. 15 and Fig. 9). Predictions for unknown patterns are considered as being positive, while predictions for known patterns are considered as being negative. The actual answer labels are also mapped such that data for known patterns

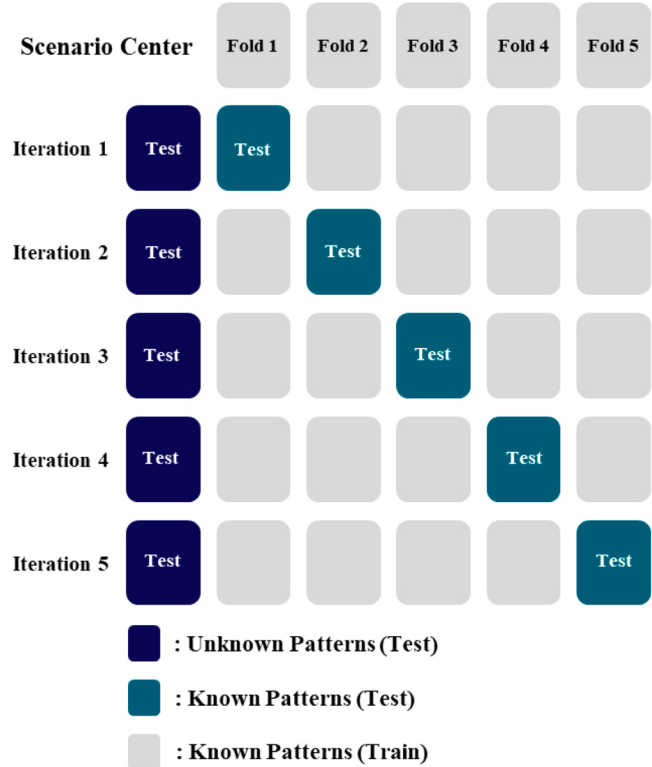


Fig. 10. Data set construction process for cross-validation.

is assigned as a negative label, while data for unknown patterns is assigned as a positive label, even if multiple new classes arise. For example, in the "Center" scenario, if the model predicts a "Center" pattern sample as an unknown pattern, it is classified as a True Positive. Conversely, if the model predicts it as a known pattern, it is counted as a False Negative. In this scenario, for other patterns assumed as known patterns (e.g., "Donut," "Loc," "Scratch," etc.), if the model predicts them as known patterns, they are classified as True Negative, while predicting them as unknown patterns in a False Positive.

Generally, when evaluating the performance of models for classes not present in training data, such as in generalized zero-shot learning,

Table 6

Performance Recall of the proposed model measured using cross validation.

Scenario Name	Iteration 1		Iteration 2		Iteration 3		Iteration 4		Iteration 5		Average	
	Acc	Recall	Acc	Recall								
Center	0.939	0.898	0.937	0.895	0.936	0.895	0.936	0.896	0.936	0.897	0.937	0.896
Donut	0.937	0.998	0.937	1.000	0.939	0.998	0.938	0.998	0.936	1.000	0.934	0.999
Edge-Loc	0.874	0.471	0.875	0.481	0.873	0.470	0.873	0.470	0.875	0.473	0.874	0.473
Edge-Ring	0.938	0.964	0.936	0.947	0.935	0.946	0.935	0.946	0.935	0.946	0.936	0.946
Loc	0.902	0.540	0.903	0.542	0.900	0.542	0.900	0.540	0.901	0.537	0.901	0.540
Random	0.939	1.000	0.938	1.000	0.938	1.000	0.942	1.000	0.936	1.000	0.939	1.000
Scratch	0.910	0.210	0.908	0.205	0.909	0.207	0.907	0.203	0.906	0.209	0.908	0.207
Near-full	0.936	1.000	0.934	1.000	0.937	1.000	0.934	1.000	0.935	1.000	0.935	1.000
Average (Macro)											0.92	0.76

the commonly used metrics are the accuracy of seen classes and the accuracy of unseen classes (Pourpanah et al., 2020). Similarly, in OSR studies, which aim to accurately detect untrained classes, the detection accuracy of unseen classes is frequently used to measure model performance (Yue et al., 2021). As can be seen in Eq. 15, the accuracy of the unknown class is synonymous with the recall of the unknown class. Therefore, in this study, we measured performance using the recall metric of the unknown class, a term more commonly used in general classification performance.

Another reason why the recall metric of the unknown class is important is that the detection accuracy of the unknown class is particularly crucial in semiconductor manufacturing processes. Since the unknown class does not exist in the training data, it is very difficult to detect newly occurring unknown defect patterns in the test data through classifiers trained with the existing training data. In semiconductor manufacturing processes, vast amounts of data are generated daily, and production proceeds through random sampling. Failure to detect such unknown defect patterns can pose significant risks to quality. For these reasons, we used the recall metric (unknown class detect accuracy) of the unknown class as the performance evaluation metric in this study.

However, if hyperparameters are adjusted solely to increase the recall metric, there is a risk of excessively detecting many normal samples due to data imbalance and known defect patterns, thereby significantly increasing inspection costs. Therefore, the overall classification accuracy of the data was also presented. This accuracy is similar to the concept of Open Set Overall Accuracy proposed in the study by Pal et al. (2022), considering both the accuracy of known classes and the accuracy of unknown classes to represent the overall performance of the model.

$$\text{Accuracy} = \frac{TP + TN}{\text{Total number of samples}}, \text{Recall} = \frac{TP}{\text{Number of unknown class samples}} \# \quad (15)$$

Table 5 presents the performance of the proposed EEOC-SVM model as demonstrated in the study. This performance was achieved using datasets constructed based on the defect pattern scenarios depicted in Fig. 8. As shown in Table 5, the EEOC-SVM achieved an average overall classification accuracy of 0.92 and a recall (classification accuracy for

unknown defect types) of 0.76 across all unknown defect pattern scenarios. Notably, in scenarios where defect patterns such as "Donut", "Random", and "Near-full" were assumed to be unknown defect patterns, the model successfully detected unknown defect types contained within the test data with an accuracy of 0.94 and a recall of 1.00. Additionally, in scenarios where defect patterns such as "Center" and "Edge-Ring" were assumed to be unknown defects, the model demonstrated excellent performance with recall metrics and classification accuracy exceeding 0.90.

In this study, we utilized a 5-fold cross-validation technique to ensure the reliability of the performance evaluation results for the proposed model. This allowed us to verify the performance variation due to randomness. The experimental design for the 5-fold cross-validation can be seen in Fig. 10. As seen in Fig. 10 shows that we first divide the known defect pattern data from one scenario dataset in Fig. 8 into a total of 5 folds. Then, we sequentially change each fold using a 'leave-one-out' method to alter the test data. At this point, the data assumed to be unknown defect patterns are not split into training and test sets, but 100 % of all data is always included only in the test data. As a result, we conduct a total of 5 repeated experiments for each scenario dataset in Fig. 8, measuring the model's performance variation due to changes in training data using the cross-validation technique. The overall model performance measured through cross-validation can be seen in Table 6. Looking at the 5-fold cross-validation results of the proposed model, we can see that the performance for each iteration is maintained without significant deviation in both accuracy and recall. Furthermore, comparing the classification performance proposed in Table 5 with the performance confirmed through cross-validation in Table 6, we can see that there is little performance variation between iterations for the data scenarios, and the average performance is also identical at about 0.92

and 0.76. These results are due to the fact that in the process of creating the test dataset, the unknown defect types are always 100 % included in the test data, minimizing the intervention of randomness by not using random splitting. Additionally, the known pattern samples used for model training are mapped to the "known pattern" class without considering subclasses, forming a single large decision boundary for the known pattern class. Therefore, if the number of samples in the training

Table 7

Performance comparison by feature-extraction method: Accuracy (Recall).

Scenario Name	Performance Comparison by Feature-Extract Method: Accuracy (Recall)					
	A	B	C	D	E	F (Proposed)
Center	0.71 (0.30)	0.83 (0.63)	0.90 (0.85)	0.81 (0.45)	0.85 (0.87)	0.94 (0.90)
Donut	0.81 (0.25)	0.86 (0.63)	0.90 (0.99)	0.85 (0.86)	0.86 (1.00)	0.94 (1.00)
Edge-Loc	0.68 (0.28)	0.77 (0.27)	0.83 (0.38)	0.79 (0.42)	0.79 (0.44)	0.88 (0.48)
Edge-Ring	0.67 (0.30)	0.70 (0.28)	0.75 (0.26)	0.84 (0.80)	0.74 (0.38)	0.94 (0.95)
Loc	0.67 (0.10)	0.79 (0.19)	0.87 (0.58)	0.79 (0.26)	0.83 (0.64)	0.90 (0.54)
Random	0.66 (0.59)	0.86 (0.99)	0.90 (1.00)	0.85 (0.88)	0.86 (1.00)	0.94 (1.00)
Scratch	0.74 (0.33)	0.82 (0.05)	0.88 (0.25)	0.83 (0.23)	0.84 (0.34)	0.91 (0.21)
Near-full	0.74 (0.71)	0.86 (1.00)	0.90 (1.00)	0.85 (1.00)	0.85 (1.00)	0.94 (1.00)
Average (Macro)	0.71 (0.40)	0.81 (0.51)	0.87 (0.66)	0.83 (0.61)	0.83 (0.71)	0.92 (0.76)

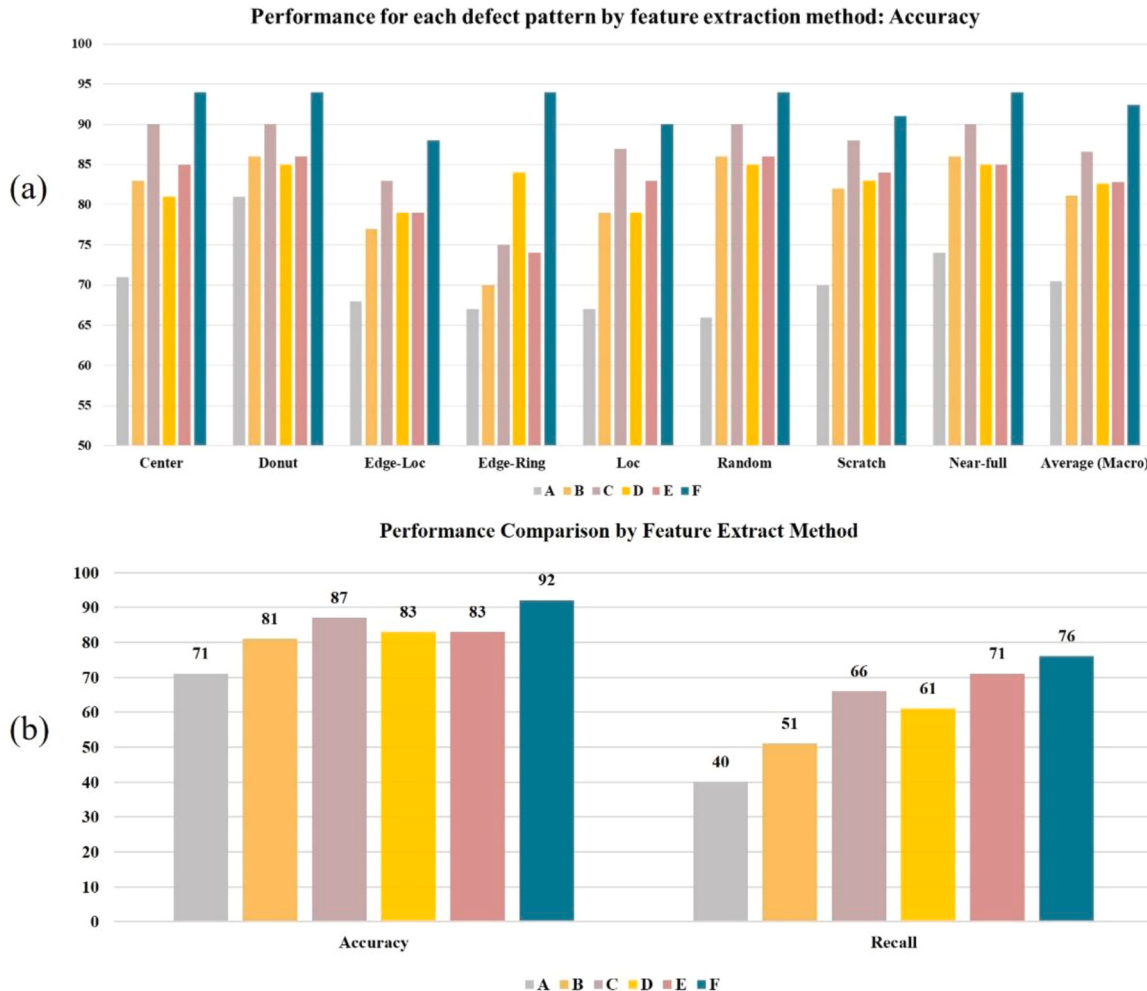


Fig. 11. (a) Accuracy performance (%) for each pattern, (b) macro-average performance (%) of accuracy and recall for all patterns.

data and the distribution between known pattern classes are maintained, we can see that performance variation due to randomness is minimized, ensuring consistent reliability in the performance evaluation process of this study.

3.7. Performance Comparison by Feature-Extract Method

In this section, we compared the performance of the proposed EEOC-SVM methodology with various WBM feature extraction methods from Table 2 and CNN-based auto-encoders using outlier detection techniques. The comparison was made using the accuracy and recall metrics presented in Eq. 15. Detailed descriptions of each compared model are

as follows:

- A. **Autoencoder (64):** A CNN-based approach to processing WBM with input-data dimensions scaled to 80×80 pixels. This model uses an end-to-end automated feature-extraction technology built on an encoder-decoder architecture to extract 64-dimensional features from the input image using a CNN kernel with learned weights. Using an encoder trained on known defect-pattern data, unknown defect patterns within the test data were detected using anomaly detection.
- B. **Before Feature Extract (6400):** The WBM image that has undergone only C-mean filtering is smoothed to one dimension and used to train

- OC-SVM.** The size of the WBM before flattening is 80×80 , and after the flattening process, it becomes a **6400**-dimensional vector.
- C. Radon/Geometry/Density (59):** After processing the WBM images with a C-mean filter, features were extracted using a combination of the Radon transform, geometric analysis, and density measurements (total **59**-dimensional vector). Subsequently, these features were used to train **OC-SVM**.
- D. Geometry (6):** The WBM defect-pattern image was analyzed as a sparse matrix, and the geometric features of the largest connected component in the WBM were used as the features (radius, area, and length of major axis of connected component (**6**-dimensional vector)). A six-dimensional vector consisting of the minor-axis length, eccentricity, and solidity was used as the input for the **OC-SVM**.
- E. Density (13):** After processing the WBM image using the C-means filter, the WBM was divided into 13 zones (**13**-dimensional vector), and features were extracted by measuring the density of the zones. These features were then used to train the **OC-SVM**.
- F. Proposed Method (20):** After processing the WBM images with a C-mean filter, 20 features (**20**-dimensional vectors) were extracted by interpolating the average values of each row from the matrices based on the Radon transform. These features were used to train the proposed model (**EEOC-SVM**).

In this section, to ensure consistent performance evaluation across models, different training datasets were used for each scenario while keeping the model's basic structure, operational method, and hyper-parameters (e.g., optimizer and learning rate of the Autoencoder, nu of SVM, etc.) unchanged. Thus, the experiments in this section evaluate how well the proposed EEOC-SVM methodology, the feature extraction methods of WBM models, and outlier detection-based autoencoder models can classify various shapes of unknown defect patterns using only known pattern data. Regarding this, the row labeled "Center" in **Table 7** represents the classification performance of each comparative model evaluated using the dataset from the "Center" scenario in **Fig. 8**. In this scenario, the "Center" defect pattern is assumed as an unknown pattern, thus excluded from the training data while all other patterns in WM-811K are included as known defect patterns.

Table 7 and **Fig. 11** show that the proposed EEOC-SVM methodology (F) has superior overall classification accuracy and recall compared with the other models. This indicates that EEOC-SVM can exhibit exceptional performance in detecting unknown defect patterns, even when only known defect patterns are used as training data. These results represent a significant advancement in overcoming existing limitations in the WBM research field. Each defect pattern is assumed to be unknown for each model; the performance per defect pattern (**Fig. 11(a)**) and average performance graph for all defects (**Fig. 11(b)**) are as shown in **Fig. 11**. In particular, the significant performance difference in specific defect patterns, such as 'Edge-Ring' and 'Random' suggests that the proposed method is better at understanding and classifying specific defect patterns. However, for defect patterns such as 'Loc' and 'Scratch', a relatively lower performance is observed compared to other models. If these

defect patterns are not trained, they are frequently confused with similarly shaped classes of trained defect patterns, such as 'Edge-Loc' or 'Loc', and the performance metrics are observed to degrade across all models.

Compared with other models, the low performance of traditional weight-based model-training techniques and anomaly-detection approaches in detecting unknown patterns highlights the limitations of these models (Model A). Although the basic performance of the OC-SVM (Model B) without feature extraction was relatively high, it still fell short of the proposed EEOC-SVM methodology. Additionally, the performance degradation experienced by Model C, which used various feature-extraction methods, and Model D, which excessively reduced the dimensionality of the original data, suggests that having too many or too few features can be disadvantageous for classifying wafer-defect patterns. Conversely, Model E, which utilized a density-estimation method for feature extraction, showed higher recall values than the other models but still performed lower in both accuracy and recall compared to the proposed EEOC-SVM methodology. This indicates that the proposed EEOC-SVM methodology is a more suitable approach for detecting unknown defect patterns.

3.8. Performance comparison by OSR model

To evaluate the performance of the proposed model more specifically, we constructed classifiers for unknown defect patterns in the WBM using various OSR techniques and compared their performance with the proposed methodology. The performance metrics compared were the same as in **Eq. (15)**. When evaluating the accuracy and recall metrics for each model, we assessed them using a binary classification approach for known and unknown classes. Detailed descriptions of the configurations of each model are as follows:

Soft-Max (80 × 80): To detect unknown patterns, we used the ResNet50 model for training. Throughout the training process, the optimal threshold for each class was determined. The model was structured to classify samples as unknown defect patterns if they failed to meet the optimal threshold for any class, based on the probability output for each class through SoftMax across all classes.

Pre-SoftMax (80 × 80): By utilizing known defect patterns, we employed logit values immediately before the SoftMax layer of a pre-trained ResNet50 model. We measured the average activation distance between each logit value. We established a threshold based on the distance between the average logits for each class of samples. This enabled us to construct a model capable of detecting unknown defect patterns.

Open-Max (80 × 80): The OpenMax model also utilizes a pre-trained ResNet50, leveraging known defect patterns. It calculates the average activation distance for each logit and then, for each class, uses the samples that are furthest away to determine the extreme values. These extreme values are then fitted to a Weibull distribution for each class. The samples that do not meet the threshold determined by the Weibull distribution are classified as having unknown defect patterns.

VGG16 & GMM (40): ([Frittoli et al., 2022](#)) used a pre-trained SSCN

Table 8
Performance comparison by OSR model: Accuracy (Recall).

Scenario Name	Performance comparison by OSR model: Accuracy (Recall)				
	Soft-Max (Nguyen et al., 2015)	Pre-SoftMax	OpenMax (Bendale and Boult, 2016)	VGG16 + GMM (Frittoli et al., 2022)	Proposed Method
Center	0.81 (0.40)	0.82 (0.43)	0.72 (0.61)	0.85 (0.69)	0.94 (0.90)
Donut	0.85 (0.42)	0.89 (0.37)	0.89 (0.35)	0.61 (0.86)	0.94 (1.00)
Edge-Loc	0.81 (0.44)	0.86 (0.43)	0.72 (0.47)	0.75 (0.39)	0.88 (0.48)
Edge-Ring	0.82 (0.13)	0.59 (0.30)	0.71 (0.42)	0.57 (0.33)	0.94 (0.95)
Loc	0.82 (0.50)	0.86 (0.43)	0.75 (0.57)	0.69 (0.43)	0.90 (0.54)
Random	0.83 (0.53)	0.78 (0.52)	0.85 (0.45)	0.74 (0.39)	0.94 (1.00)
Scratch	0.80 (0.37)	0.87 (0.36)	0.81 (0.50)	0.58 (0.21)	0.91 (0.21)
Near-full	0.85 (0.14)	0.87 (0.11)	0.87 (0.14)	0.90 (0.82)	0.94 (1.00)
Average (Macro)	0.82 (0.37)	0.82 (0.37)	0.79 (0.44)	0.71 (0.52)	0.92 (0.76)

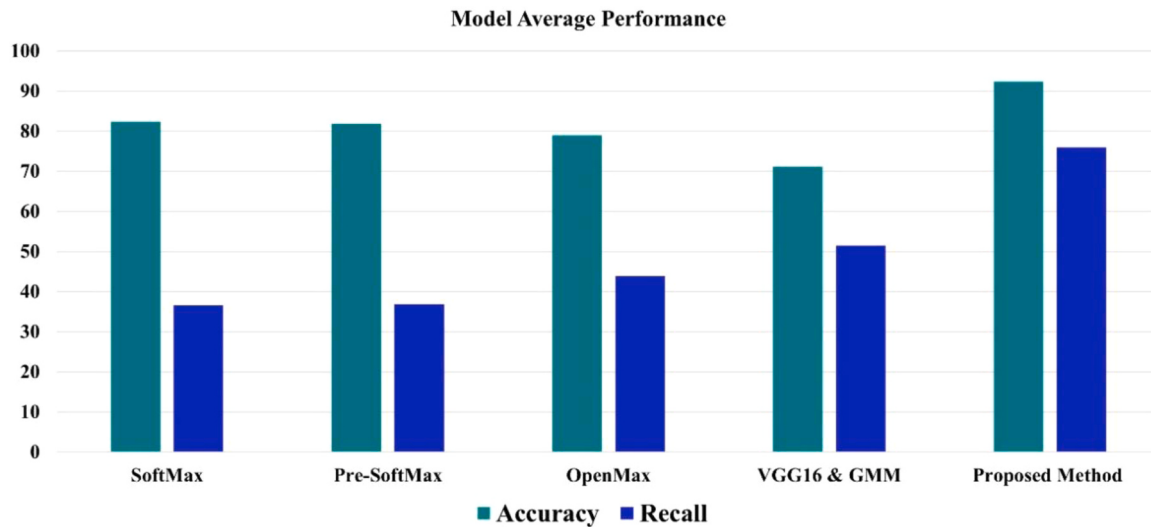


Fig. 12. Macro average performance (%) of each OSR model.

Table 9
Real field data images and number of samples.

Defect Pattern Name	Wafer Map Image	Number of Samples
Eye		715
Windmill		221
Total		936

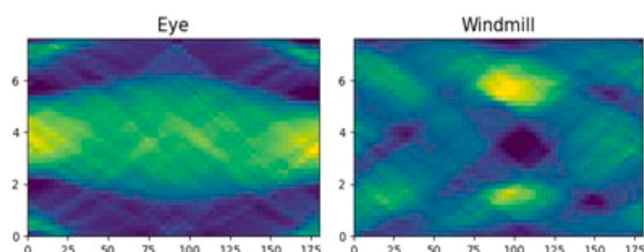


Fig. 13. Sinogram image of real field data.

model based on a 224×224 VGG16 on a $20,000 \times 20,000$ WDM, leveraging known defect pattern classes. This model reduced the features to 128 dimensions, and these reduced features were then used as inputs to a GMM, which is also trained on known defect-pattern classes. The density-based likelihood ratio from the GMM was used to detect unknown classes. In our study, we used WBM instead of WDM and therefore employed the VGG16 model for dimension reduction instead of the SSCN module. In addition, we reduced the number of features to **40 dimensions** instead of 128, which were then used as inputs for the GMM.

Proposed Method (20): After processing the WBM images with a C-mean filter, 20 features (**20-dimensional vectors**) were extracted by interpolating the average values of each row from the matrices based on the Radon transform. These features were used to train the proposed

model (EEOC-SVM).

Table 8 presents a comparison of the classification performance of the proposed model and models developed using different OSR techniques. The methodology leveraging EEOC-SVM proposed in this study demonstrates superior classification accuracy and recall metrics across most unknown defect-pattern datasets, except for the recall of the 'Scratch' and 'Local' classes. For defect patterns such as 'Scratch', 'Loc', and 'Edge-Loc', this study assumed unknown defect patterns using the WM-811K dataset in leave-one-out method. However, because these defects are highly similar, even without training with one class assumed to be unknown, the models tend to recognize them as having similar defect patterns, resulting in a generally low recall performance across all models. Models based on Soft-Max, Pre-SoftMax, and Open-Max, which use pre-trained deep-learning classifier thresholds for each defect pattern, show marginally higher recall metrics for distinguishing similar patterns.

In contrast, for single defect patterns that differ significantly from existing defect patterns, such as 'Center', 'Donut', 'Edge-Ring', 'Random', and 'Near-full', a noticeable difference exists in the accuracy and recall metrics between other OSR techniques and the proposed methodology. In particular, for defect patterns such as 'Edge-Ring', the proposed model exhibits a recall rate over 50 % higher than that of the next-best-performing model, Open-Max, indicating a significant improvement. The test performance of each model also shows that the ResNet-based Open-Max, SoftMax, and Pre-SoftMax models exhibit similar performance. **Fig. 12** presents a graph of the classification accuracy and macro-averaged recall metrics for all datasets for each model using the OSR technique. The OSR method using Vgg16 and GMM shows slightly better recall metrics compared to other models. However, the proposed method outperforms this model by approximately 25 % in recall and about 21 % in accuracy. Additionally, compared to all models, the proposed method achieves at least 10 % higher accuracy and at least 24 % higher recall. These results demonstrate the effectiveness and superior performance of the proposed approach for detecting unknown defect patterns within the WBM domain.

Case Study 2: using real-field data

This section further verifies the applicability of the methodologies for effectively detecting various unknown defect patterns that can occur during the semiconductor-manufacturing process, based on real field data obtained from real semiconductor-production sites. The defect pattern images obtained from real field data and their counts are listed in **Table 9**.

The 'Eye' defect pattern is considered as a new single-defect pattern, having a shape similar to a mix of the 'Center' and 'Edge-Ring' defect

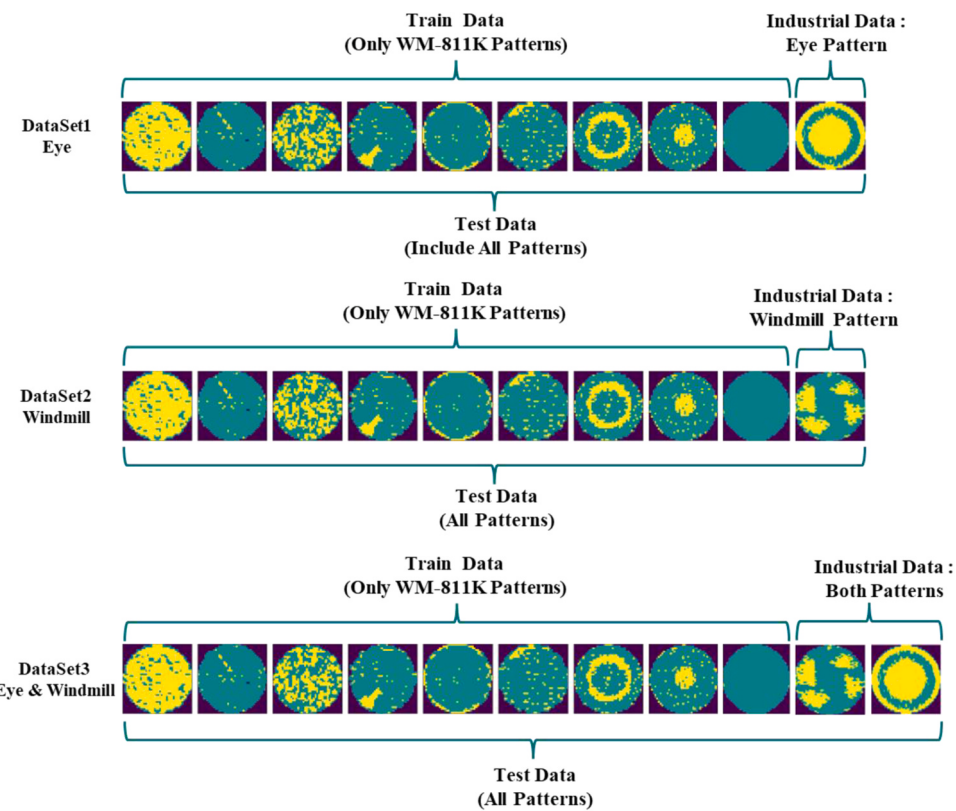


Fig. 14. Dataset construction process with real field data.

Table 10
Performance comparison by OSR method: accuracy and recall.

Model Name	Dataset1 Eye		Dataset2 Windmill		Dataset3 Eye & Windmill		Average (Macro)	
	Accuracy	Recall	Accuracy	Recall	Accuracy	Recall	Accuracy	Recall
Soft-Max (Nguyen et al., 2015)	0.80	0.62	0.85	0.67	0.78	0.59	0.81	0.63
Pre-SoftMax	0.72	0.56	0.86	0.71	0.70	0.69	0.71	0.65
OpenMax (Bendale and Boult, 2016)	0.75	0.50	0.80	0.44	0.72	0.42	0.76	0.45
VGG16 + GMM (Frittoli et al., 2022)	0.80	0.61	0.81	0.71	0.79	0.71	0.80	0.68
Proposed Method	0.98	1.00	0.98	1.00	0.98	1.00	0.98	1.00

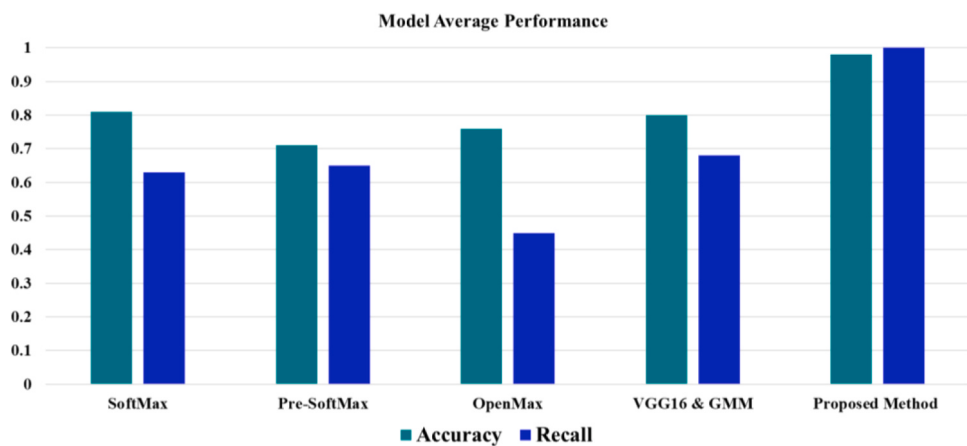


Fig. 15. Macro average performance (%) of each model.

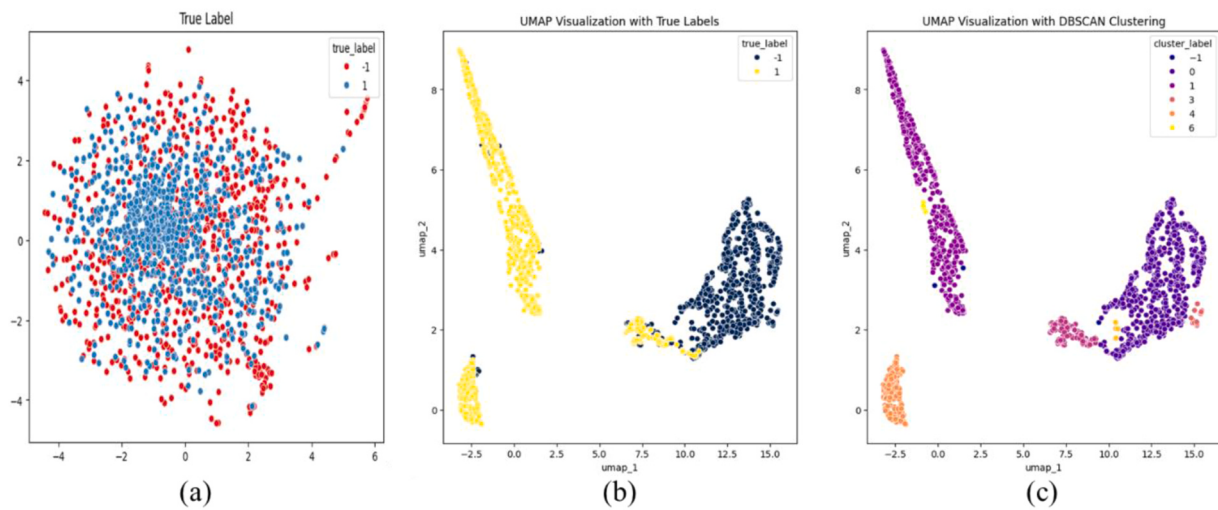


Fig. 16. (a) True labels after classification by OC-SVM, (b) true labels after classification by EEOC-SVM, (c) DB-SCAN clustering results after classification by EEOC-SVM.

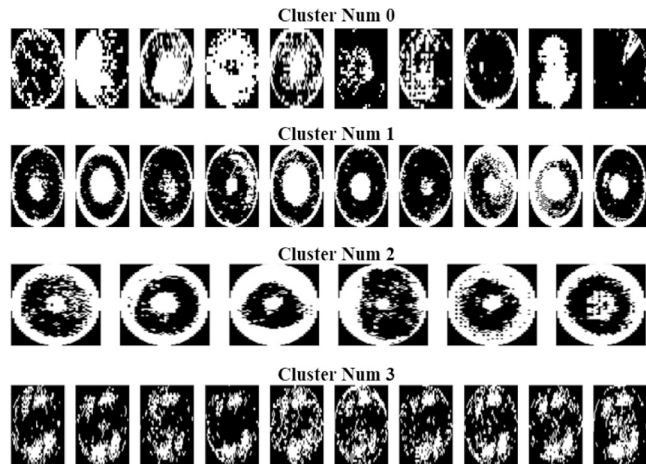


Fig. 17. WBM image for each cluster using the results from DB-SCAN.

patterns found in WM-811K. The 'Windmill' defect image is similar to the 'Loc' defect pattern but is characterized by the continuous occurrence of four 'Loc' defect patterns at a specific location. The sinogram images after the Radon transform of each industrial dataset can be observed in Fig. 13, showing different patterns of defect characteristics from those of WM-811K.

As seen in Fig. 14, the model was trained using only the WM-811K dataset, and experiments were designed to evaluate the model's performance by adding three different combinations of datasets to the test data. Dataset 1 includes the addition of the "Eye" pattern to the test data, and Dataset 2 includes the addition of the "Windmill" pattern. Each dataset is constructed by adding industrial defect patterns to the test data alongside the defect patterns from the WM-811K dataset. Additionally, Dataset 3 includes both the "Eye" and "Windmill" patterns in the test data, allowing for the evaluation of the model's performance in scenarios where multiple unknown defect patterns occur simultaneously.

Table 10 and Fig. 15 present the classification performance of various OSR techniques applied under the same conditions as in Section 4, utilizing a real-field dataset. A closer examination of the results revealed similarities to those evaluated using the WM-811K data in Section 4. The models employing OSR techniques on the same ResNet50 model, namely SoftMax, OpenMax, and Pre-SoftMax, exhibited an

average accuracy difference of less than 5 %, indicating no significant difference in classification performance. However, the SoftMax model, which learned the optimal threshold for each class from the training data, demonstrated a marginally better performance in terms of accuracy and recall than the other models. Similarly, the models utilizing VGG16 and GMM with OSR techniques, as in Section 4, show the highest recall metrics. However, no significant difference was observed in the accuracy when compared with the other models.

Moreover, in evaluation dataset3 (Eye and Windmill), which assumes the occurrence of multiple unknown defect-pattern classes, all models except for the proposed methodology showed a decrease in classification accuracy compared to datasets 1 and 2. This suggests that the performance of the model may decline when the number of unknown defect patterns increases or when various defect patterns occur simultaneously. However, the proposed EEOC-SVM model demonstrated superior performance in terms of both accuracy and recall, proving its efficient defect-pattern detection and classification capabilities on actual field data. Notably, the ability of this model to detect 100 % of the unknown defect patterns and achieve an overall accuracy of over 98 % in all datasets indicates that it can effectively identify and classify various defect patterns in real-field environments, as well as manage the emergence of multiple unknown defect patterns simultaneously.

The results of the visual analysis of the test data using the additional clustering methods are presented in Fig. 16. Fig. 16 (a) shows the results of classifying the test data using OC-SVM without going through the feature-extraction phase on industrial dataset3 (which contains two unknown defect patterns), and then visualizing the samples predicted as unknown defect patterns using UMAP with the actual answer labels of each sample. Here, the "1" and "-1" labels represent unknown and known defect patterns, respectively. Fig. 16 (b) shows the results using the answer labels of the unknown defect patterns finally predicted by the EEOC-SVM using the proposed methodology, and (c) shows the results of each cluster formed using DB-SCAN on the unknown defect patterns predicted by the EEOC-SVM in the same manner. Thus, we can confirm that the proposed method can effectively detect both known and unknown patterns, and clear cluster separation among unknown defect patterns is also observed.

Additionally, by examining the WBM images of the samples in each cluster based on the clustered results in Fig. 16(c), as shown in Fig. 17, we can confirm that different types of defect patterns are appropriately formed for each cluster: cluster 0 (known type of defect pattern), clusters 1 and 2 ("Eye" defect pattern), and cluster 3 ("Windmill" defect pattern). These results indicate that even with the occurrence of multiple

unknown defect patterns, by separating unknown data using the proposed methodology and EEOC-SVM and proceeding with clustering based on the results, engineers can be assisted with early recognition of the emergence of new types of defects. Furthermore, the results demonstrate the potential of the model to efficiently handle tasks, such as adding classes of unknown defect patterns to existing classifiers or labeling new defects.

4. Conclusions

This study proposes a methodology for accurately and efficiently detecting unknown defect patterns that have been overlooked in previous WBM defect-pattern analysis studies. Most previous studies focused on the use of training datasets to make classifiers more accurate and efficient. However, these studies did not consider the possibility and importance of detecting unknown defect patterns that do not exist in the training data and have recently emerged. Consequently, it is a major challenge to detect, collect, and label these unknown defect patterns at semiconductor manufacturing sites.

Therefore, this study proposes an EEOC-SVM model and methodology that utilizes OSR techniques to accurately classify known defect patterns without any information or assumptions regarding unknown defect patterns. This methodology includes designing a model that combines C-mean filtering for noise removal in the WBM, feature extraction based on the Radon transform, and the EEOC-SVM model to improve the decision uncertainty of the traditional OC-SVM. To evaluate the performance of the proposed model, we assumed each defect pattern in the WM-811K dataset to be an unknown pattern and compared its performance with that of existing WBM feature-extraction methods and anomaly-detection techniques using a weighted learning-based CNN model. The results showed that the proposed EEOC-SVM model exhibited the highest performance in terms of both accuracy and recall rates, and successfully detected unknown defect patterns. Additionally, by constructing models applying various OSR techniques and conducting detection evaluations for unknown defect patterns in WBM under the same conditions, the proposed model demonstrated superior classification performance across all metrics. Furthermore, this study proved that the proposed model could efficiently detect and classify various defect patterns in real environments, surpassing an overall accuracy of 98 % and achieving 100 % detection of unknown defect patterns in all datasets based on actual semiconductor-manufacturing field data ('Eye', 'Windmill'). This confirms that the model can not only efficiently detect and classify various defect patterns that may occur in real environments but is also applicable to situations where multiple unknown defects emerge simultaneously. In addition, we visually analyzed the test data using additional clustering methods, confirming that the proposed method can effectively detect known and unknown data, and observed a clear clustering separation between the unknown data. Consequently, the proposed methodology is expected to significantly affect the quality control and maintenance of future semiconductor-manufacturing processes, which will become more complex. This methodology can be used as a powerful tool for effectively detecting and responding to unexpected defect patterns.

This study aims to clearly detect unknown defect data, which are new defect types that have not been pre-learned. Accordingly, the test data were divided into known defect pattern data and unknown defect pattern data, but the detailed classes of the known defect pattern sample were not classified. Therefore, future research, based on the results of this study, is focusing on updating the pre-trained classifier using a stream-based online active learning method. This will ensure that the pre-trained classifier maintains high performance on known defect pattern data while continuously detecting newly occurring unknown defect pattern data in the test data. Additionally, in order to better understand more detailed defect information, we are conducting multi-task learning research that combines defect pattern classifiers and language models using text data containing information about suspicious

processes and equipment, as well as WBM images. These studies will contribute significantly to semiconductor manufacturing processes by not only detecting unknown defects proposed in this study but also providing a clearer and more detailed analysis of the causes of existing defects.

CRediT authorship contribution statement

Beom-Seok Kim: Visualization, Validation, Software, Formal analysis. **Min-Joo Kim:** Project administration, Data curation. **Jin-Su Shin:** Writing – original draft, Validation, Methodology, Conceptualization. **Donghee Lee:** Supervision, Project administration, Conceptualization.

Declaration of Competing Interest

The authors declare that they have no known competing financial interests or personal relationships that could have appeared to influence the work reported in this paper.

Acknowledgement

This work was supported by the National Research Foundation of Korea (NRF) grant funded by the Korea government (MSIT) (No. NRF-2022R1C1C1011743).

Data availability

Data will be made available on request.

References

- Batool, U., Shapiai, M.I., Tahir, M., Ismail, Z.H., Zakaria, N.J., Elfakharany, A., 2021. A Systematic review of deep learning for silicon wafer defect recognition. *IEEE Access* 9, 116572–116593. <https://doi.org/10.1109/ACCESS.2021.3106171>.
- Bendale, A., Boult, T.E., 2016. Towards open set deep networks. *Proc. IEEE Conf. Comput. Vis. Pattern Recognit.* 1563–1572.
- Cha, J., Jeong, J., 2022. Improved U-net with residual attention block for mixed-defect wafer maps. *Appl. Sci. (Switz.)* 12 (4). <https://doi.org/10.3390/app12042209>.
- Chen, F.-L., Liu, S.-F., 2000. A neural-network approach to recognize defect spatial pattern in semiconductor fabrication. *IEEE Trans. SEMICONDUCTOR Manuf.* 13 (3).
- Chen, S., Zhang, Y., Hou, X., Shang, Y., Yang, P., 2022. Wafer map failure pattern recognition based on deep convolutional neural network. *Expert Syst. Appl.* 209. <https://doi.org/10.1016/j.eswa.2022.118254>.
- Fan, S.K.S., Chiu, S.H., 2024. A new ViT-Based augmentation framework for wafer map defect classification to enhance the resilience of semiconductor supply chains. *Int. J. Prod. Econ.* 273. <https://doi.org/10.1016/j.ijpe.2024.109275>.
- Frittoli, L., Carrera, D., Rossi, B., Fragneto, P., Boracchi, G., 2022. Deep open-set recognition for silicon wafer production monitoring. *Pattern Recognit.* 124. <https://doi.org/10.1016/j.patcog.2021.108488>.
- Geng, C., Huang, S.J., Chen, S., 2021. Recent Advances in Open Set Recognition: A Survey. In: *IEEE Transactions on Pattern Analysis and Machine Intelligence*, 43. IEEE Computer Society, pp. 3614–3631. <https://doi.org/10.1109/TPAMI.2020.2981604>.
- Hou, X., Yi, M., Chen, S., Liu, M., Zhu, Z., 2024. Recognition and classification of mixed defect pattern wafer map based on multi-path DCNN. *IEEE Trans. Semicond. Manuf.* 37 (3), 316–328. <https://doi.org/10.1109/TSIM.2024.3418520>.
- Hsu, C.Y., Chen, W.J., Chien, J.C., 2020. Similarity matching of wafer bin maps for manufacturing intelligence to empower Industry 3.5 for semiconductor manufacturing. *Comput. Ind. Eng.* 142. <https://doi.org/10.1016/j.cie.2020.106358>.
- Hsu, S.C., Chien, C.F., 2007. Hybrid data mining approach for pattern extraction from wafer bin map to improve yield in semiconductor manufacturing. *Int. J. Prod. Econ.* 107 (1), 88–103. <https://doi.org/10.1016/j.ijpe.2006.05.015>.
- Hyun, Y., Kim, H., 2020. Memory-augmented convolutional neural networks with triplet loss for imbalanced wafer defect pattern classification. *IEEE Trans. Semicond. Manuf.* 33 (4), 622–634. <https://doi.org/10.1109/TSIM.2020.3010984>.
- Júnior, P.R.M., Boult, T.E., Wainer, J., & Rocha, A. (2016). Open-Set Support Vector Machines. <https://doi.org/10.1109/TSMC.2016.2574496>.
- Kang, H., Kang, S., 2021. A stacking ensemble classifier with handcrafted and convolutional features for wafer map pattern classification. *Comput. Ind.* 129. <https://doi.org/10.1016/j.compind.2021.103450>.
- Kim, E.S., Choi, S.H., Lee, D.H., Kim, K.J., Bae, Y.M., Oh, Y.C., 2021. An oversampling method for wafer map defect pattern classification considering small and imbalanced data. *Comput. Ind. Eng.* 162. <https://doi.org/10.1016/j.cie.2021.107767>.
- Kim, M., Tak, J., Shin, J., 2023. A deep learning model for wafer defect map classification: perspective on classification performance and computational volume. *Phys. Status Solidi (B) Basic Res.* <https://doi.org/10.1002/pssb.202300113>.

- Kim, T., Behdinan, K., 2023. Advances in machine learning and deep learning applications towards wafer map defect recognition and classification: a review. In: In *Journal of Intelligent Manufacturing*, 34. Springer, pp. 3215–3247. <https://doi.org/10.1007/s10845-022-01994-1>.
- Kyeong, K., Kim, H., 2018. Classification of mixed-type defect patterns in wafer bin maps using convolutional neural networks. *IEEE Trans. Semicond. Manuf.* 31 (3), 395–402. <https://doi.org/10.1109/TSM.2018.2841416>.
- Lee, H., Kim, H., 2020. Semi-supervised multi-label learning for classification of wafer bin maps with mixed-type defect patterns. *IEEE Trans. Semicond. Manuf.* 33 (4), 653–662. <https://doi.org/10.1109/TSM.2020.3027431>.
- Lee, J.H., Moon, I.C., Oh, R., 2021. Similarity search on wafer bin map through nonparametric and hierarchical clustering. *IEEE Trans. Semicond. Manuf.* <https://doi.org/10.1109/TSM.2021.3102679>.
- Liao, C.S., Hsieh, T.J., Huang, Y.S., Chien, C.F., 2014. Similarity searching for defective wafer bin maps in semiconductor manufacturing. *IEEE Trans. Autom. Sci. Eng.* 11 (3), 953–960. <https://doi.org/10.1109/TASE.2013.2277603>.
- Mahdavi, A., & Carvalho, M. (2021). A Survey on Open Set Recognition. *Proceedings - 2021 IEEE 4th International Conference on Artificial Intelligence and Knowledge Engineering, AIKE 2021*, 37–44. <https://doi.org/10.1109/AIKE52691.2021.00013>.
- Nag, S., Makwana, D., R, S.C.T., Mittal, S., Mohan, C.K., 2022. WaferSegClassNet - A light-weight network for classification and segmentation of semiconductor wafer defects. *Comput. Ind.* 142. <https://doi.org/10.1016/j.compind.2022.103720>.
- Nakazawa, T., Kulkarni, D.V., 2018. Wafer map defect pattern classification and image retrieval using convolutional neural network. *IEEE Trans. Semicond. Manuf.* 31 (2), 309–314. <https://doi.org/10.1109/TSM.2018.2795466>.
- Nakazawa, T., Kulkarni, D.V., 2019. Anomaly detection and segmentation for wafer defect patterns using deep convolutional encoder-decoder neural network architectures in semiconductor manufacturing. *IEEE Trans. Semicond. Manuf.* 32 (2), 250–256. <https://doi.org/10.1109/TSM.2019.2897690>.
- Nguyen, A., Yosinski, J., & Clune, J. (2015). Deep Neural Networks are Easily Fooled: High Confidence Predictions for Unrecognizable Images. <https://doi.org/10.48550/arXiv.1412.1897>.
- Piao, M., Jin, C.H., Lee, J.Y., Byun, J.Y., 2018. Decision tree ensemble-based wafer map failure pattern recognition based on radon transform-based features. *IEEE Trans. Semicond. Manuf.* 31 (2), 250–257. <https://doi.org/10.1109/TSM.2018.2806931>.
- Pourpanah, F., Abdar, M., Luo, Y., Zhou, X., Wang, R., Lim, C.P., Wang, X.-Z., & Wu, Q. M.J. (2020). A Review of Generalized Zero-Shot Learning Methods. <https://doi.org/10.1109/TPAMI.2022.3191696>.
- Saqlain, M., Jargalsaikhan, B., Lee, J.Y., 2019. A voting ensemble classifier for wafer map defect patterns identification in semiconductor manufacturing. *IEEE Trans. Semicond. Manuf.* 32 (2), 171–182. <https://doi.org/10.1109/TSM.2019.2904306>.
- Shim, J., Kang, S., Cho, S., 2020. Active learning of convolutional neural network for cost-effective wafer map pattern classification. *IEEE Trans. Semicond. Manuf.* 33 (2), 258–266. <https://doi.org/10.1109/TSM.2020.2974867>.
- Shinde, P.P., Pai, P.P., Adiga, S.P., 2022. Wafer defect localization and classification using deep learning techniques. *IEEE Access* 10, 39969–39974. <https://doi.org/10.1109/ACCESS.2022.3166512>.
- Wu, M.J., Jang, J.S.R., Chen, J.L., 2015. Wafer map failure pattern recognition and similarity ranking for large-scale data sets. *IEEE Trans. Semicond. Manuf.* 28 (1), 1–12. <https://doi.org/10.1109/TSM.2014.2364237>.
- Xu, Q., Yu, N., Essaf, F., 2022. Improved wafer map inspection using attention mechanism and cosine normalization. *Machines* 10 (2). <https://doi.org/10.3390/machines10020146>.
- Yu, J., Liu, J., 2021. Two-dimensional principal component analysis-based convolutional autoencoder for wafer map defect detection. *IEEE Trans. Ind. Electron.* 68 (9), 8789–8797. <https://doi.org/10.1109/TIE.2020.3013492>.
- Yu, J., Lu, X., 2016. Wafer Map Defect Detection and Recognition Using Joint Local and Nonlocal Linear Discriminant Analysis. *IEEE Trans. Semicond. Manuf.* 29 (1), 33–43. <https://doi.org/10.1109/TSM.2015.2497264>.
- Yu, N., Xu, Q., Wang, H., 2019. Wafer defect pattern recognition and analysis based on convolutional neural network. *IEEE Trans. Semicond. Manuf.* 32 (4), 566–573. <https://doi.org/10.1109/TSM.2019.2937793>.
- Yue, Z., Wang, T., Sun, Q., Hua, X.S., Zhang, H., 2021. Counterfactual zero-shot and open-set visual recognition. *Proc. IEEE/CVF Conf. Comput. Vis. Pattern Recognit.* 15404–15414.
- Zhang, X., Jiang, Z., Yang, H., Mo, Y., Zhou, L., Zhang, Y., Li, J., Wei, S., 2024. DMWMNet: A novel dual-branch multi-level convolutional network for high-performance mixed-type wafer map defect detection in semiconductor manufacturing. *Comput. Ind.* 161. <https://doi.org/10.1016/j.compind.2024.104136>.
- Zhu, F., Yang, J., Gao, C., Xu, S., Ye, N., Yin, T., 2016. A weighted one-class support vector machine. *Neurocomputing* 189, 1–10. <https://doi.org/10.1016/j.neucom.2015.10.097>.
- Zhu, J., Liu, J., Xu, T., Yuan, S., Zhang, Z., Jiang, H., Gu, H., Zhou, R., Liu, S., 2022. Optical wafer defect inspection at the 10 nm technology node and beyond. In: In *International Journal of Extreme Manufacturing*, 4. Institute of Physics. <https://doi.org/10.1088/2631-7990/ac64d7>.